ACS OMEGA

Open Access

http://pubs.acs.org/journal/acsodf

Article

Base-Directed Formation of Isostructural Lanthanide–Sulfate–Glutarate Coordination Polymers with Photoluminescence

Saranphong Yimklan,*,# Nippich Kaeosamut,# Nithiwat Sammawipawekul, Sutsiri Wongngam, Satienrapong Ngamsomrit, Apinpus Rujiwatra, and Yothin Chimupala*,#

Cite This: *ACS Omega* 2024, 9, 3988–3996

Read Online

ACCESS | Metrics & More | Article Recommendations | Supporting Information

ABSTRACT: A series of five isostructural 3D lanthanide-based coordination polymers $[Ln^{III}_2(H_2O)_6(glu)(SO_4)_2]_n$ [Ln = Pr(**1**), Nd(**2**), Sm(**3**), Eu(**4**), and Gd(**5**)] was effortlessly obtained within a few minutes via the microwave-heating method. The employment of auxiliary bases, that is, sodium hydroxide, 4,4′-bipyridine, and 1,4-diazabicyclo[2.2.2]octane, led to the formation of the title complex, whereas base-free synthesis yielded a three-dimensional inorganic coordination polymer, $[Ln_2(H_2O)_4(SO_4)_3]_n{\cdot}nH_2O$, Ln = Nd (**2a**). The robustness of the synthetic method was illustrated as both microwave-heating and conventional hydrothermal techniques also enabled the formation of a high-crystalline phase-pure complex **1**–**5**. In the structure of **1**–**5**, glutarato (glu^{2-}) and sulfato ligands link dinuclear Ln(III) building units into three-dimensional frames. The glu^{2-} ligands act as tethering linkers, expanding the structure into a neutral 3D coordination network. Hydrogen bonds were found to be the predominant intermolecular interactions in the crystal structures. Photoluminescence of the complex **1**–**5** was studied.

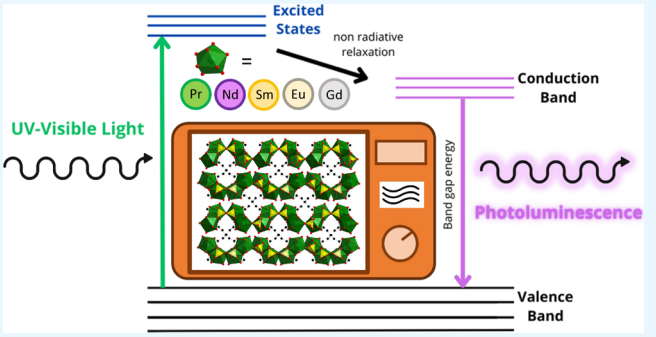

INTRODUCTION

Coordination polymers (CPs) and metal–organic frameworks (MOFs) have been attracted by materials chemists, especially in the recent two decades, because of their provable and tunable potential applications[1] such as catalysis,[2,3] gas adsorption and separation,[4,5] magnetism,[6] sensing,[7−9] photoluminescence,[10−13] and so on. Among these functional CPs and MOFs, coordination polymers of the *not-so-rare* earth[14] lanthanides (Ln-CPs) are of great interest due to their fantastic coordination diversity and potentially applicable magnetic, catalytic, and photoluminescence properties.[15−19] Also, the rational synthesis of Ln-CPs and MOFs with desired functionality is, indeed, a great challenge because their crystalline phase formations depend on the coordination chemistry of metal centers, coordination as well as the acid–base nature of linkers, synthetic technique, and synthetic parameters such as solvent, temperature, pH, and stoichiometry.[20,21] The synthetic methods can be one of the key factors that contribute to the formation of the aimed structures.[20] In this work, we employed the microwave-heating method proven as an alternative route toward new coordination polymeric compounds compared with the conventional hydrothermal method, using water as a green solvent. Due to the fact that the ionic radii of lanthanide cations are relatively larger than those of first-row transition metals, they can offer accessible coordination sites with diverse coordination geometries that allow the formation of fascinating new architecture with intrinsic photoluminescence and/or magnetic properties.[22−25] The luminescence of trivalent lanthanide (Ln^{3+}) cations is offered by intraconfigurational f–f transitions, which often show luminescence in the regions of visible or near-infrared light upon irradiation with ultraviolet radiation.[26−30] The photoluminescence properties of Ln^{3+} are intrinsically emerging due to their electronic configuration [Xe] $4f^n$, which carries a large set of electronic energy levels. Because the core 4f levels are shielded by the filled $5s^25p^6$ subshells, these energy levels are thus defined. Each Ln^{3+} cation has, therefore, a sharp fingerprint photoluminescence spectrum. Lanthanide-based coordination polymers may enable potential applications in sensing for stimuli, such as temperature and chemicals, that influence the luminescence properties.[31,32] In the context of crystal engineering, the intrinsic nature of organic linkers, such as molecular flexibility, coordination modes, connectivity, point of extension, size, and functional factors, such as

Received: October 27, 2023
Revised: December 6, 2023
Accepted: December 8, 2023
Published: January 8, 2024

aromaticity functional groups, are crucial for linker selection.[33,34] Glutarate (glu^{2-}) anion is a flexible linker from the full deprotonation of glutaric acid ($HOOC(CH_2)_3COOH$, H_2glu) that can adopt different coordination modes.[35−37] The flexibility in the molecular conformation of the chain-like aliphatic carboxylate, like glu^{2-}, leads to an unprecedented topological structure that, sometimes, leads to fascinating properties.[38] There are several Ln-CPs with glutarate as a key organic linker reported up-to-date, such as $\{[Nd(H_2O)_4(glu)]\text{-}Cl\}_n$[39,40] and $\{[Nd_2(H_2O)_2(glu)_3]\cdot 2H_2O\}_n$.[41] Auxiliary organic ligands are often introduced into the coordination entity in order to promote the antenna effect, which directly coordinates to Ln^{3+} cation and enhances Ln^{3+} emission by using their intrinsic chromophore nature of the π-conjugated aromatic system,[26,42,43] such as in $[Eu^{III}(BSA)(glu)(H_2O)_2]_n$ [Ln = Eu, Sm, Ce, Pr, Nd; HBSA = benzenesulfonic acid],[44] $[Ln^{III}(glu)\text{-}(pic)(H_2O)_2]_n$ [Ln = Sm, Tb and Eu]; Hpic = picolinic acid],[45] $[Ln^{III}_2(H_2O)_2(ip)(glu)_2]_n$ [Ln = Gd, Dy, Y; H_2ip = isophthalic acid], and $[Sm_2(H_2O)_2(ip)(glu)_2]_n$.[46] The lanthanide and group 3 element coordination polymers with glu^{2-} and 1,10-phenanthroline as auxiliary chelating ligands $[Ln\text{-}(phen)(glu)Cl]_n$ [Ln = Y, Tm; phen = 1,10-phenanthroline], $[Ln_2(phen)_2(glu)_3]_n$ [Ln = Ce, Tb, Ho], and $[La_2(glu)_3(H_2O)_3]_n$ exhibited the effects of auxiliary organic ligands on their photoluminescence properties.[26] Divalent sulfate anion was found to be one of the inorganic building blocks and auxiliary ligand for the supporting strength of the inorganic layer structure in the ionic coordination polymers of $\{[4,4'\text{-bipyH}_2][La(SO_4)_2]\cdot 2H_2O\}_n$,[47] $[Eu_3(2,6\text{-pdc})_3(2,6\text{-Hpdc})(SO_4)(H_2O)_3]_n$, $[Ln_2(2,6\text{-pdc})_2(SO_4)(H_2O)_2]_n$ [Ln = Ce, Pr, Nd, Sm], and $[Ce_5(2,6\text{-pdc})_6(SO_4)_2(H_2O)_3\cdot(Me_2NH_2)]_n$ [2,6-pdcH$_2$ = pyridine-2,6-dicarboxylic acid].[48]

Herein, we report a synthetic exploration of new lanthanide−sulfate−glutarate coordination polymers of the early lanthanides using a flexible *chain-like* glu^{2-} as an organic spacer. The influences of the base, as well as various synthetic techniques, on the phase formation were studied. From the identical synthetic conditions with only the presence/absence of a base, two coordination polymers, formulated as $[Ln_2(H_2O)_6(glu)(SO_4)_2]_n$ [Ln = , Pr(**1**), Nd(**2**), Sm(**3**), Eu(**4**), Gd(**5**)] and $[Nd_2(H_2O)_4(SO_4)_3]_n\cdot nH_2O$, **2a**, emerged. Photoluminescence of the reported Ln-CPs has also been studied and reported herein.

RESULTS AND DISCUSSION

Synthesis and Structural Description of 1−5. Five isostructural lanthanide-based coordination polymers $[Ln_2(H_2O)_6(\mu_4\text{-glu})(\mu_3\text{-}SO_4)_2]_n$ (Ln = Pr, **1**; Nd, **2**; Sm, **3**, Eu, **4**; Gd, **5**) were successfully and effortlessly synthesized using the microwave-heating method. As a representative of the series, a single crystal of $[Gd^{III}_2(H_2O)_6(\mu_4\text{-glu})(\mu_3\text{-}SO_4)_2]_n$, **5**, was selected for X-ray single-crystal structure analysis. The crystallographic information and structural refinements of **5**, compared to its reported congener, $[Nd^{III}_2(H_2O)_6(\mu_4\text{-glu})(\mu_3\text{-}SO_4)_2]_n$, discovered by our group,[49] are listed in Table 1. Note that the unit cell parameters of **5** (Gd) are relatively smaller than that of **2** (Nd) due to lanthanide contraction found in ordinary lanthanide CPs and MOFs.[26] The X-ray crystal structure revealed that the titled coordination polymers crystallize in the monoclinic $P2_1/c$ space group. Unambiguously, there are two crystallographically independent trivalent Gd(III) atoms in the asymmetric unit; both are coordinated to nine crystallographically unique oxygen atoms: three glutarate ligands, three different sulfate anions, and three aqua ligands adopted in the *distorted tricapped trigonal-prismatic* coordination geometry, *TPRS*-$\{Gd^{III}O_9\}$. The Gd−O bond distances are 2.331(5)−2.825(7) Å, comparable to the related reported polymeric structures.[50,51] These are relatively shorter than those Nd−O bonds found in its neodymium congener, **2** (Nd), that is in the range of 2.383(2)−2.785(2) Å, since Gd^{3+} has smaller atomic radii than Nd^{3+} (see Tables S1 and S3). There are two crystallographically unique μ_3-sulfato ligands with identical coordination modes, μ_3-*sulfato*-$\kappa^1O{:}\kappa^1O'{:}\kappa^1O''$ or [3.1110], present in the structure, as shown in the asymmetric unit (see Figure 1a,c). The inorganic assembly by edge-sharing *TPRS*-$\{Gd^{III}O_9\}$ polyhedrons linked with the μ_3-sulfate ligands ends up with an infinite polymeric layer of $\{Gd_2(H_2O)_6(SO_4)_2\}_n^{2n+}$ cation that paralleled to the (011) layers. These cationic sheets comprise large inorganic $\{Gd(SO_4)\}_4$ rings that are stabilized by hydrogen-bonding interactions between the ligating aqua and the bridging sulfato ligands (see Figure 2). The hydrogen-bonding interaction parameters of **5** are given in Table S4. The formation of a three-dimensional coordination network is eventually enabled by connecting the adjacent cationic $\{Gd_2(H_2O)_6(SO_4)_2\}_n^{2n+}$ sheets by the bridging glutarato ligands (see Figure 3). The bridging glutarate anion is bound in the uncommon chelating bridge mode of μ_4-*glutarato*-$\kappa^1O{:}\kappa^2O'{:}\kappa^1O''{:}\kappa^2O'''$, as depicted in Figure 1c. The conformation of glutarate ligands about C−C bonds is all staggered with an *anti*−*anti* conformation and with torsion angles of about C1−C2−C3−C4, 155.9(2)°, and C2−

Table 1. Crystal Data and Structure Refinement for 2a and 5 Compared with Those of 2 as Reported in the Reference[a]

identification code	**2** (ref 49)	**2a** (this work)	**5** (this work)
CCDC No.	CCDC 2107848	CSD 2303320	CCDC 2302504
empirical formula	$C_5H_{18}Nd_2O_{18}S_2$	$H_{10}Nd_2O_{17}S_3$	$C_5H_{18}Gd_2O_{18}S_2$
temperature/K	298(2)	293(2)	298(2)
crystal system	monoclinic	monoclinic	monoclinic
space group	$P2_1/c$	$P2_1/c$	$P2_1/c$
a/Å	15.5461(1)	13.8068(4)	15.4247(2)
b/Å	12.6621(1)	9.5985(3)	12.5175(2)
c/Å	8.8883(1)	10.2682(4)	8.8101(2)
β/°	95.287(1)	100.050(3)	95.513(2)
volume/Å^3	1742.19(3)	1339.91(8)	1693.17(5)
Z	4	4	4
crystal size/mm^3	0.3 × 0.3 × 0.1	0.39 × 0.38 × 0.3	0.33 × 0.3 × 0.18
radiation	MoKα (λ = 0.71073)	MoKα (λ = 0.71073)	MoKα (λ = 0.71073)
2θ range for data collection/°	4.156 to 54.888	5.196 to 54.702	4.198 to 54.912
reflections collected	38711	27754	22904
independent reflections	3830[R_{int} = 0.0667, R_{sigma} = 0.0381]	2796[R_{int} = 0.2200, R_{sigma} = 0.0824]	3660[R_{int} = 0.0454, R_{sigma} = 0.0849]
goodness-of-fit on F^2	1.061	1.039	1.037
final R indexes [$I \geq 2\sigma(I)$]	R_1 = 0.0240, wR_2 = 0.0502	R_1 = 0.0761, wR_2 = 0.1880	R_1 = 0.0638, wR_2 = 0.0500
final R indexes [all data]	R_1 = 0.0282, wR_2 = 0.0536	R_1 = 0.0944, wR_2 = 0.2409	R_1 = 0.0764, wR_2 = 0.0683

[a] $R_1 = \sum||F_0| - |F_c||/\sum|F_0|$ and $wR_2 = [\sum w(F_0^2 - F_c^2)^2/\sum wF_o^4]^{1/2}$ for $F_0^2 > 2\sigma(F_0^2)$.

https://doi.org/10.1021/acsomega.3c08506
ACS Omega 2024, 9, 3988−3996

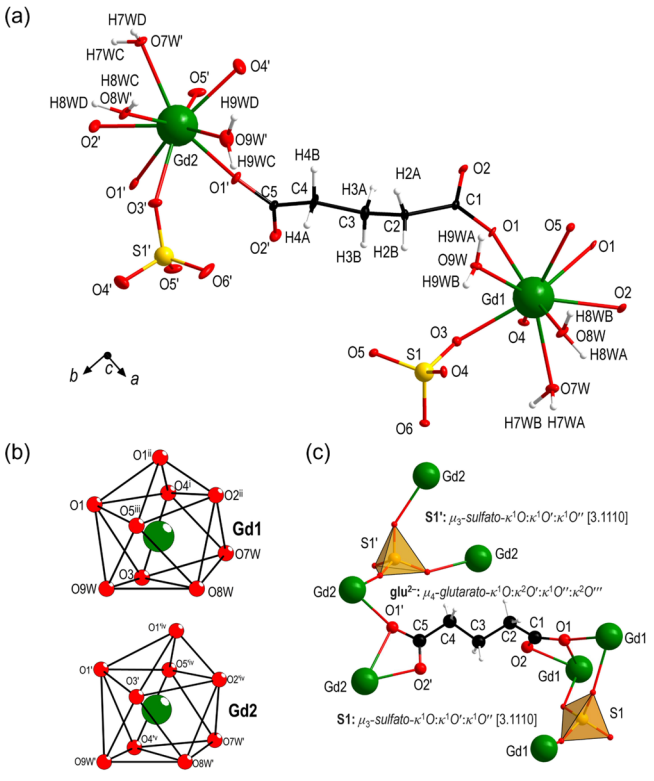

Figure 1. (a) Extended asymmetric unit of $[Gd_2(H_2O)_6(glu)(SO_4)_2]_n$, **5**, showing the coordination environment with displacement ellipsoids at the 50% probability level. (b) Polyhedral representations illustrating coordination geometries of the two crystallographically unique *TPRS*-$\{Gd^{III}O_9\}$, Gd1 and Gd2, in **5**. (c) Coordination modes of glutarato and sulfato ligands in **5**.

C3−C4−C5, 173.8(1)°. As depicted in Figure 3b,c, the bridging glutarato ligand cross-linked the adjacent inorganic *gadolinium-sulfato*-$\{Gd_2(H_2O)_6(SO_4)_2\}_n^{2n+}$ sheets that were solely made from crystallographically related trivalent gadolinium (Gd1 or Gd2), causing the packing of the cationic layers in ABAB··· fashion along the *b*- and *c*-axes of the unit cell.

The X-ray crystal structure of $[Gd_2(H_2O)_6(\mu_4\text{-glu})(\mu_3\text{-}SO_4)_2]_n$, **5**, as described above, can be definitely a representative of the well-washed and dried bulk crystalline solids obtained from the rapid microwave-heating synthesis as the well-indexed powder X-ray diffraction (PXRD) pattern compared with the calculated patterns of **5**, as shown in Figure 4a and supported by elemental microanalysis. The presence of glutarate and sulfate in the structure was affirmed by Fourier transform infrared (FTIR) spectroscopy (see Figure S1). The asymmetric and the symmetric stretching bands, ν_{as}(C═O) and ν_s(C═O), of carboxyl groups in **5** (Gd) are at 1538 and 1443 cm^{-1}, respectively, whereas the stretching band of sulfate ($\nu_{as}(SO_4^{2-})$) is at 1104 cm^{-1}.[52] These ν(C═O) bands are slightly blue-shifted compared to the stretching bands found in the neodymium congener (complex **2**, ν_{as}(C═O) at 1533 cm^{-1} and ν_s(C═O) at 1431 cm^{-1}).

The identical microwave-heating synthetic conditions were applied to the early lanthanide congeners, that is, praseodymium (Pr), neodymium (Nd), samarium (Sm), and europium (Eu), using their prepared hydrated sulfate salts as starting materials. From the PXRD patterns unambiguously illustrated in Figure 4c, it is proved that the rapid microwave-heating synthesis leads to isostructural crystalline structures of $[Ln_2(H_2O)_6(\mu_4\text{-glu})(\mu_3\text{-}SO_4)_2]_n$, where Ln = Pr(**1**), Nd(**2**), Sm(**3**), Eu(**4**), and Gd(**5**). Note that the PXRD patterns were compared to the theoretical PXRD patterns of **2** (Nd) and **5** (Gd) that were calculated against the atomic position, unit cell composition, and lattice parameters of the X-ray structures of **2** (Nd, reported by our group)[49] and **5** (Gd, this work). The isostructural lanthanide coordination polymers can emerge due to the similarity in the ionic radii of the trivalent Ln^{3+} cations, as found in the other related lanthanide−glutarate series.[26,51] Since the availability of the starting materials, the neodymium coordination polymer $[Nd_2(H_2O)_6(\mu_4\text{-glu})(\mu_3\text{-}SO_4)_2]_n$ was selected for further studies on synthetic technique, the effect of bases, and thermal stability.

As the crystalline-phase purity is well indicated by PXRD patterns, thermogravimetric analysis (TGA) of **2**, as a representative example, was done in order to fulfill the chemical composition of the materials, especially the composition of combustible organic moiety and water

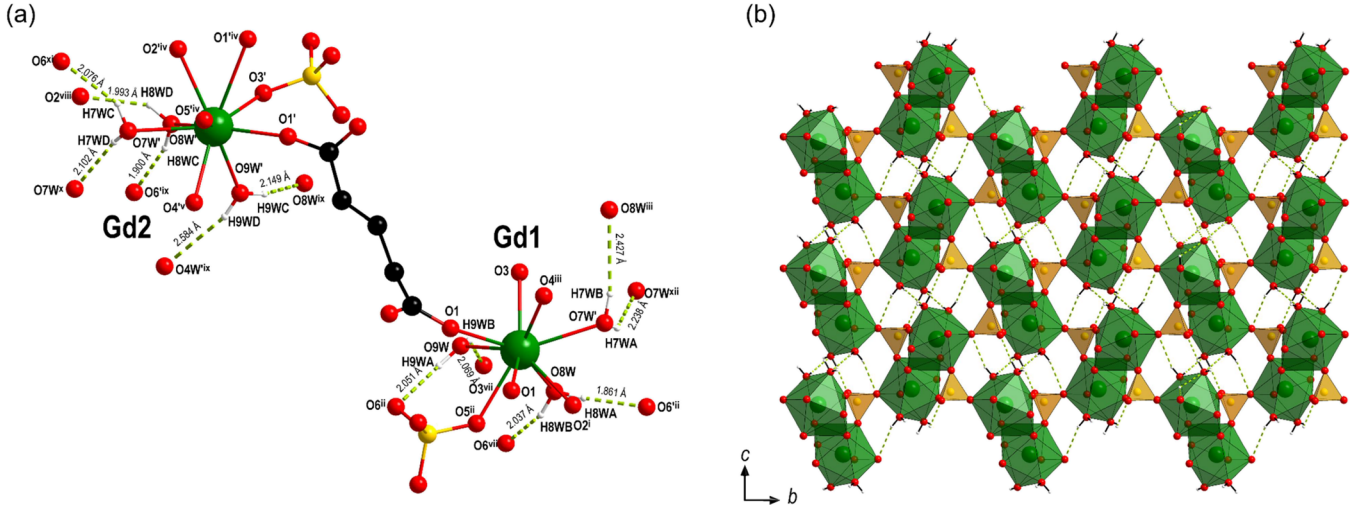

Figure 2. (a) Twelve crystallographically dependent hydrogen-bonding interactions (green dashed line) in $[Gd_2(H_2O)_6(glu)(SO_4)_2]_n$, **5**. (b) O−H···O hydrogen-bonded in a cationic 2D-$\{Gd_2(H_2O)_3(SO_4)_2\}_n^{2n+}$ layer in **5** viewed along *a*-axis.

https://doi.org/10.1021/acsomega.3c08506
ACS Omega 2024, 9, 3988−3996

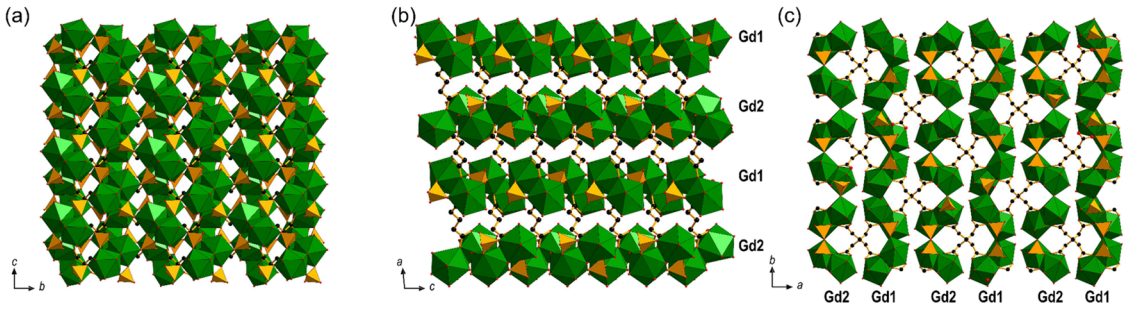

Figure 3. Graphical representation of the X-ray structure of $[Gd_2(H_2O)_6(glu)(SO_4)_2]_n$, **5**, viewed along the (a) *a*-, (b) *b*-, and (c) *c*-axis.

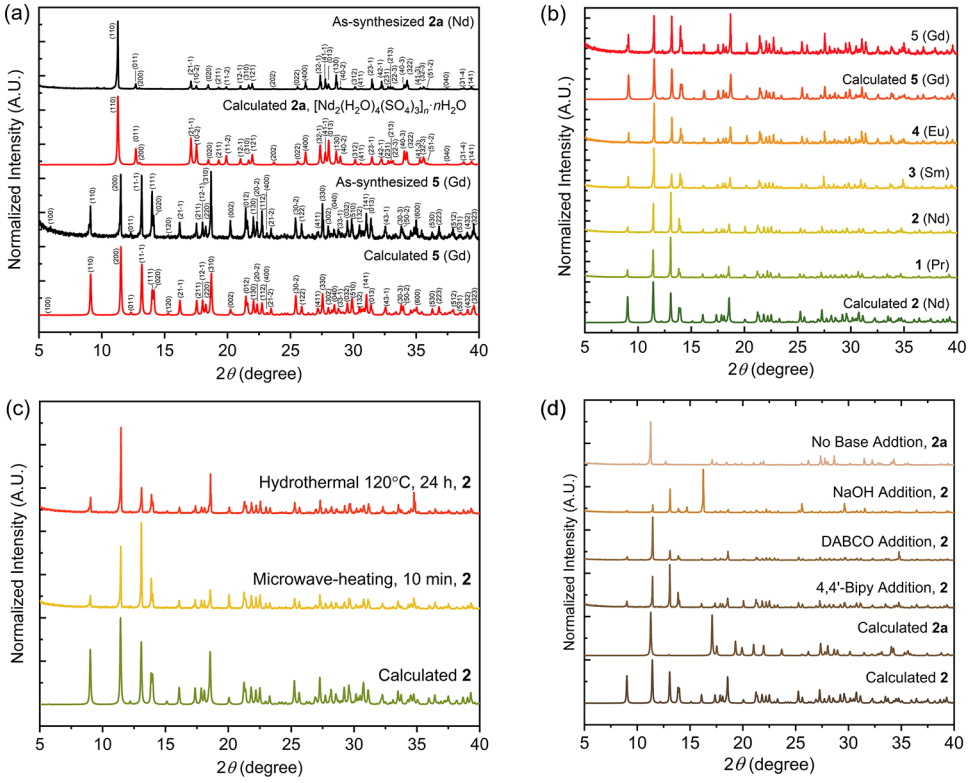

Figure 4. PXRD pattern of (a) as-synthesized $[Gd_2(H_2O)_6(glu)(SO_4)_2]_n$, **5**, and $[Nd_2(H_2O)_4(SO_4)_3]_n{\cdot}nH_2O$, **2a** (black), compared and indexed to the calculated patterns (red); (b) as-synthesized $[Ln_2(H_2O)_6(glu)(SO_4)_2]_n$, where Ln = Pr (**1**), Nd (**2**), Sm (**3**), Eu (**4**), Gd (**5**), compared to the calculated patterns; (c) bulk solid obtained from the synthesis using microwave-heating and the conventional hydrothermal method; and (d) bulk solid obtained from the synthesis with/without different base addition.

contents. TGA/DTA has been carried out under air atmosphere in the range of 40−1000 °C (see Figure S2). The net weight loss of 53.17%, which occurred at 193, 595, 645, and 927 °C, corresponds to the chemical formula $[Nd_2(H_2O)_6(C_5H_6O_4)(SO_4)_2]_n$ (calcd 53.19%). Three endothermic (193, 595, and 927 °C) peaks and one exothermic (645 °C) peak appeared in the DTA. The weight losses are due to the removal of water, sulfate, and gaseous products of the combustion of organic moieties, as the 46.83% residue is Nd_2O_3 (confirmed by PXRD, calcd 46.81%).

Synthetic Method-Independent Synthesis of 2 (Nd). The identical stoichiometric compositions of starting materials were analyzed, and then different synthetic methods were applied such as microwave-heating (identical to the above procedure) and conventional hydrothermal method at 120 °C for 24 h. As the PXRD patterns of the obtained products from both synthetic methods were well indexed against the unit cell parameters and the atomic position in the crystal structure of **2**, as shown in Figure 4, the conventional hydrothermal synthesis (24 h) and microwave-heating technique (several minutes) yielded the identical compound. Note that the average yield of the microwave-heating method (56 ± 3% yield, 10 min) was superior to that of the conventional hydrothermal method (34 ± 2% yield, 24 h). This obviously indicates that this microwave-heating method can be an alternative synthetic method for lanthanide coordination polymers that shortens the reaction time from 24 h to several minutes. Moreover, this rapid synthesis employs water, a green solvent, and can save much time and energy in coordination polymer synthesis.

Base-Directed Formation of 2 and Structural Description of 2a. In the first blueprint of crystal engineering, we honestly aimed to introduce the extended *N*-donor bidentate ligand such as 4,4′-bipyridine (4,4′-bipy) or diazabicyclo[2.2.2]octane (DABCO) into the polymeric structure. However, no such organic base is presented in the

https://doi.org/10.1021/acsomega.3c08506
ACS Omega 2024, 9, 3988−3996

final structures, as described above. Therefore, the synthesis was modified by removing the base from our synthetic recipe, and we found that the synthesis without base addition led to the formation of a new inorganic coordination polymer of $[Nd_2(H_2O)_4(\mu_4\text{-}SO_4)_3]_n{\cdot}nH_2O$, **2a,** as evidenced from the PXRD pattern in Figure 4b (top). Apart from the organic base 4,4′-bipy and DABCO, an ordinary inorganic base NaOH can also direct the phase formation of **2**. This exhibits the role of bases in the context of carboxylic acid deprotonation that drives and promotes the coordination polymer formation very well. The base-directed synthesis can be summarized in Scheme 1.

Scheme 1. Synthesis of Lanthanide−Glutarate−Sulfate Coordination Polymers Reported in This Work

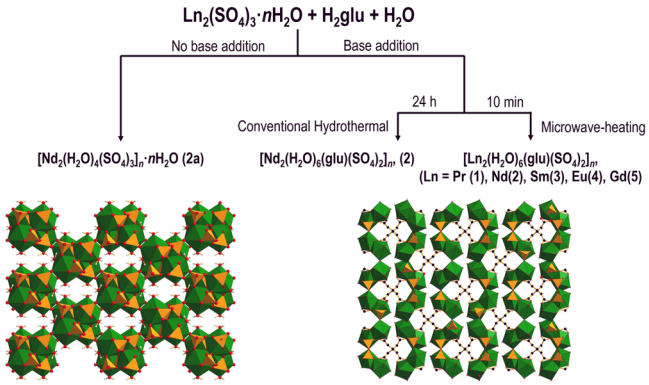

The single crystals from the synthesis without base addition were selected for further X-ray crystal analysis. Crystallographic information and structural refinements of $[Nd_2(H_2O)_4(\mu_4\text{-}SO_4)_3]_n{\cdot}nH_2O$, **2a,** are listed in Table 1. The X-ray crystal structure shows that **2a** also crystallizes in the monoclinic $P2_1/c$ space group and comprises two crystallographically unique trivalent Nd(III) in the asymmetric unit (see Figure 5a). Nd^{III} is surrounded by nine crystallographically unique oxygen atoms, seven of μ_4-sulfato oxygens and two oxygens from the two ligating waters. The Nd−O bond distances are, as listed in Table S2, found to be in the range 2.400(8)−2.782(9) Å. There are three crystallographically dependent μ_4-sulfato ligands with two types of coordination modes, that is, μ_4-*sulfato*-$\kappa^1O{:}\kappa^2O'{:}\kappa^1O''{:}\kappa^2O'''$ or [4.2211] and μ_4-*sulfato*-$\kappa^1O{:}\kappa^1O'{:}\kappa^1O''{:}\kappa^1O'''$ or [4.1111] in the crystal structure, as shown in Figure 5a,b. The edge-sharing of $\{Nd^{III}O_9\}$ building unit that is linked with the μ_4-sulfato ligands leads to an infinite polymeric 3D structure of $[Nd_2(H_2O)_4(\mu_4\text{-}SO_4)_3]_n$ that allows the formation of 1D channel along the [001] direction (see Figure 5d) for a crystallographically disordered waters of crystallization (O17W and O17W′). The crystal framework of **2a** is also hydrogen-bonding-rich as there are 14 crystallographically independent hydrogen-bonding interactions in the crystal structure (see Figure 5c). The hydrogen-bonding interaction parameters of **2a** are listed in Table S5.

Photoluminescence Properties of 1−5. As shown in Figure 6d, it can be clearly seen that Eu^{3+} in $[Eu^{III}_2(H_2O)_6(glu)(SO_4)_2]_n$, **4**, can show intense characteristic emissions from $^5D_0 \rightarrow {}^7F_J$ (J = 0, 2, 4). For Pr^{3+} in **1**, and Nd^{3+} in **2**, only weak emissions can be observed, that is, $^3P_0 \rightarrow {}^3H_J$ (J = 3, 5) (see Figure 6a,b), and for Sm^{3+} in **3**, no emission peaks were observed (see Figure 6c). As expected, the photoluminescence spectrum of Gd^{3+} in **5** exhibits $^8S \rightarrow {}^6P_{7/2}$, as shown in Figure 6e. The remarkably high energies of the excited states of Gd^{3+} ion were reported to be due to the exceptional stability of the half-filled f-shell that prevents energy transfer from ligands, which consequently causes any f−f transition unachievable.[53,54]

CONCLUSIONS

Five isostructural lanthanide-based coordination polymers, $[Ln^{III}_2(H_2O)_6(glu)(SO_4)_2]_n$ [Ln = Pr(**1**), Nd(**2**), Sm(**3**), Eu(**4**), and Gd(**5**), were successfully and rapidly synthesized by using the microwave-heating method. The phase formation of the reported coordination polymer series is found to be synthetic-method-independent and base-directed. The synthesis of **2** without base addition leads to a polymeric inorganic coordination polymer of $[Nd^{III}_2(H_2O)_4(SO_4)_3]_n{\cdot}nH_2O$. This exhibited the role of the base in the context of the protonation state of the polycarboxylic acids as organic linkers in the synthesis of lanthanide-based coordination polymers. The photoluminescence properties of the five complexes were studied.

EXPERIMENTAL SECTION

Physical Measurements. Powder X-ray diffraction (PXRD) patterns were investigated with a Rigaku SmartLab diffractometer (Mo Kα). The FT-IR spectrum was collected using a Frontier PerkinElmer FT-IR spectrometer with a universal ATR sampling accessory in the range of 4000−400 cm^{-1}. Thermogravimetric/differential scanning calorimetric analyses (TGA/DSC) were conducted using a Rigaku Thermo Plus EVO2 system. The photoluminescence spectra were collected by using an Avantes spectrophotometer (AvaSpec-2048TEC-USB2-2) with a 255 nm excitation source.

Synthesis of 1−5. Lanthanide (III) sulfate hydrate salts $Ln_2(SO_4)_3{\cdot}nH_2O$ were prepared by dissolving Pr_6O_{11} (**1**) or Ln_2O_3 (Ln = Nd, **2** and **2a**; Sm, **3**, Eu, **4**; Gd, **5**) in 6.0 M sulfuric acid and then recrystallizing and washing the obtained sulfate salts by deionized water. Glutaric acid ($C_5H_8O_4$, Sigma-Aldrich, 99%) was then added into a 0.020 M $Ln_2(SO_4)_3$ solution (5.00 mL, 0.100 mmol) in a 50 mL glass reactor or 40 mL Teflon-lined Parr autoclave. A 0.020 M base in DI water [prepared from sodium hydroxide (NaOH, Loba Chemie, 98%), 4,4′-bipy ($C_{10}H_8N_2$, Sigma-Aldrich, 98%), or DABCO (Sigma-Aldrich, >99%)] solution (5.00 mL, 0.100 mmol) was then added into the beaker. The solution was then heated by 800 W microwave irradiation for 10 min or an electric oven at 120 °C for 24 h. Crystals of **1−5** were crystallized from the reaction with base addition and then collected and stored in the mother liquor. Crystals of **2a** were crystallized from the reaction without a base addition. $[Pr_2(H_2O)_6(C_5H_6O_4)(SO_4)_2]_n$ (**1**) Yield: 31%. FT-IR (ATR, ν, cm^{-1}): 3600 (m), 3547 (m), 3501 (m), 3463 (m), 3309 (m), 3241 (m), 3167 (m), 3081 (m), 2975 (m), 2376 (w), 2189 (w), 2034 (w), 1894 (w), 1658 (m), 1528 (s), 1458 (s), 1361 (m), 1305 (m), 1207 (s), 1154 (vs), 1060 (vs), 992 (vs), 766 (s), 729 (m), 655 (s), 605 (vs), 586 (vs), 502 (s), 444 (m); $[Nd_2(H_2O)_6(C_5H_6O_4)(SO_4)_2]_n$ (**2**) Yield: 56% with microwave-heating or 34% with the conventional hydrothermal method. FT-IR (ATR, ν, cm^{-1}): 3560 (w), 3510 (w), 3464 (w), 3375 (m), 3203 (m), 3058 (w), 2932 (w), 2350 (w), 2114 (w), 2082 (w), 1918 (w), 1613 (m), 1533 (s), 1431 (s), 1354 (w), 1262 (w), 1104 (vs), 1095 (vs), 954 (m), 790 (w), 749 (w), 652 (s), 593 (vs), 499 (s), 456 (s);

https://doi.org/10.1021/acsomega.3c08506
ACS Omega 2024, 9, 3988−3996

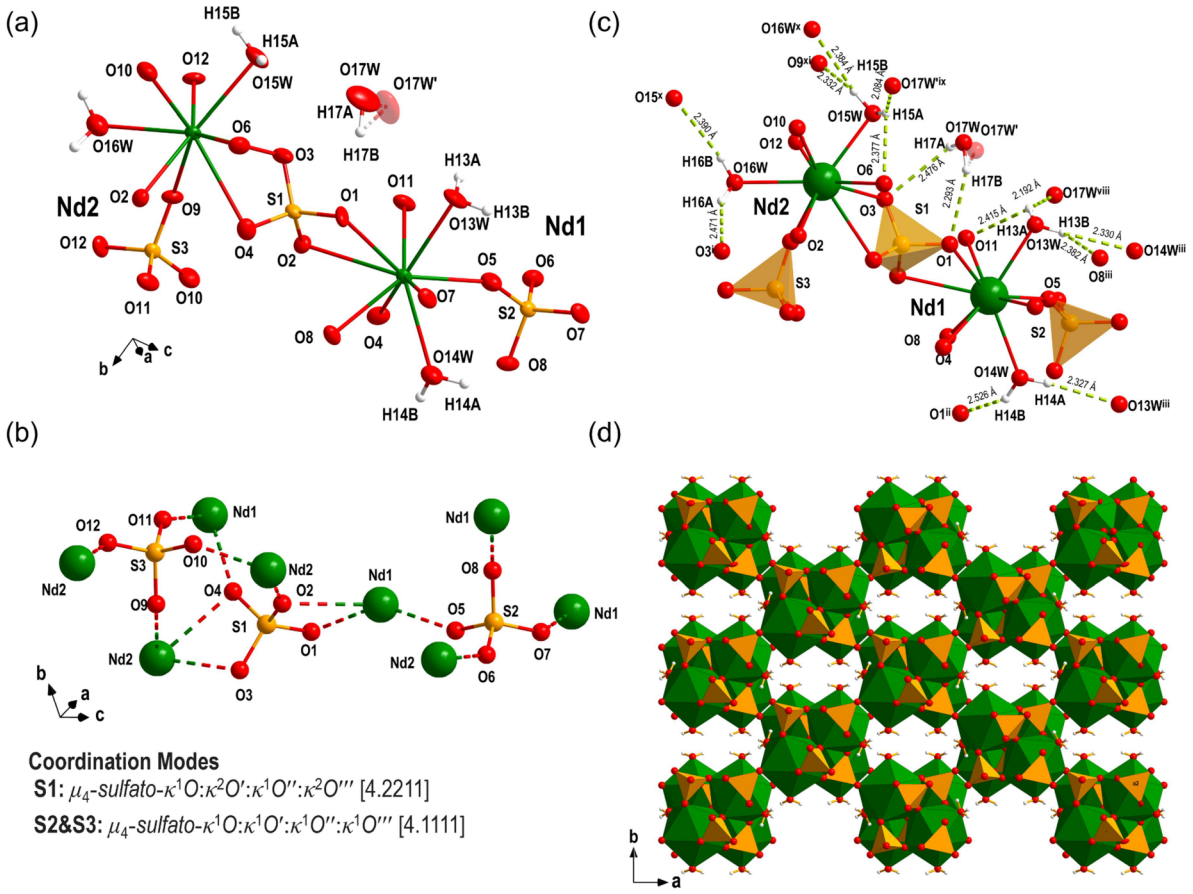

Figure 5. (a) Asymmetric unit of $[Nd_2(H_2O)_4(SO_4)_3]_n{\cdot}nH_2O$, **2a**. (b) Coordination modes of three crystallographically unique sulfato ligands in **2a**. (c) Fourteen crystallographically dependent O−H···O hydrogen-bonding interactions in **2a**. (d) Polyhedral representation of **2a**, viewed along the *c*-axis.

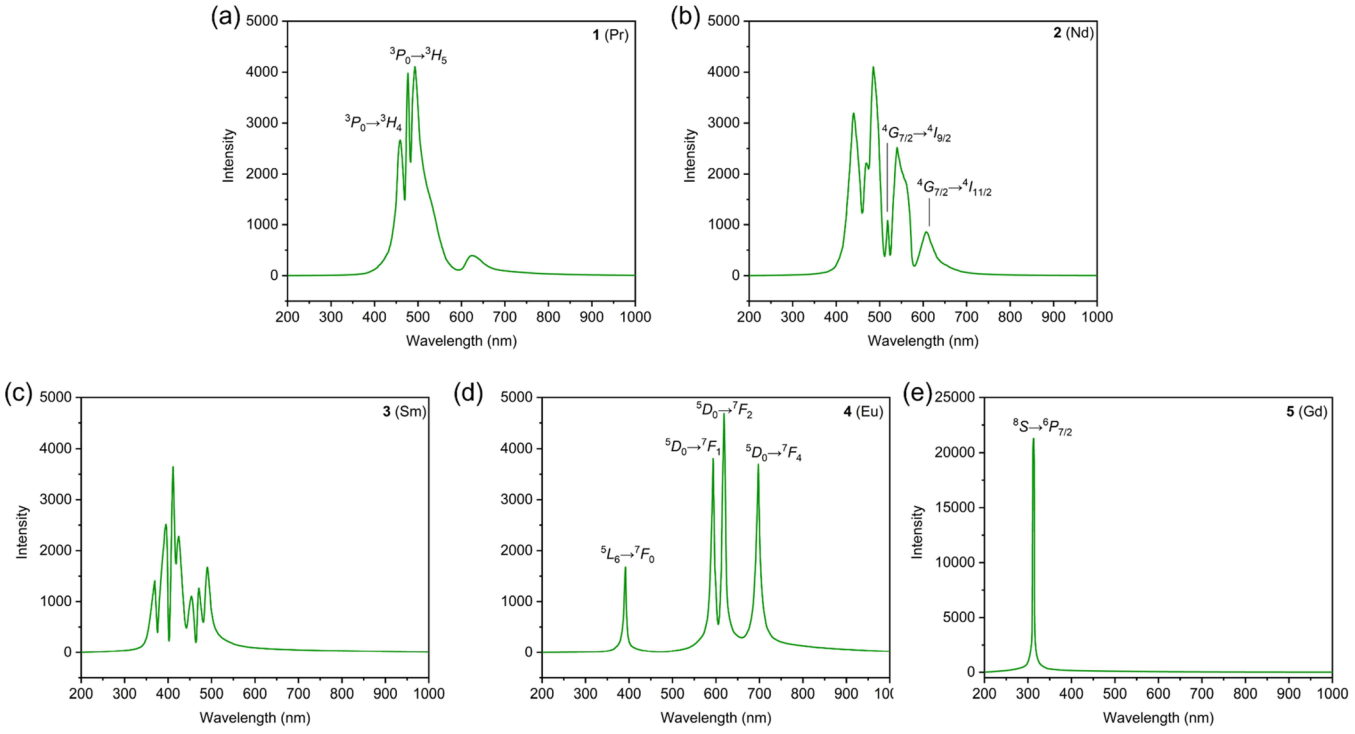

Figure 6. Photoluminescence spectra ($\lambda_{excitation}$ = 255 nm) of the as-synthesized $[Ln_2(H_2O)_6(glu)(SO_4)_2]_n$, (a) Ln = Pr (**1**), (b) Nd (**2**), (c) Sm (**3**), (d) Eu (**4**), and (e) Gd (**5**).

https://doi.org/10.1021/acsomega.3c08506
ACS Omega 2024, 9, 3988−3996

$[Nd_2(H_2O)_4(SO_4)_3]_n$ (**2a**) Yield: 40%. FT-IR (ATR, ν, cm^{-1}): 3375 (vs), 2349 (w), 2122 (w), 2085 (w), 1727 (m), 1647 (s), 1637 (s), 1341 (w), 1228 (m), 1197 (s), 1127 (vs), 1091 (vs), 1048 (vs), 1041 (vs), 1021 (vs), 971 (vs), 887 (s), 582 (vs), 535 (vs), 466 (m); $[Sm_2(H_2O)_6(C_5H_6O_4)(SO_4)_2]_n$ (**3**) Yield: 39%. FT-IR (ATR, ν, cm^{-1}): 3781 (w), 3719 (w), 3477 (m), 3373 (m), 3242 (m), 3064 (m), 2947 (w), 2349 (w), 2112 (w), 1981 (w), 1898 (w), 1621 (m), 1536 (s), 1434 (s), 1356 (m), 1264 (m), 1110 (vs), 1098 (vs), 958 (m), 792 (m), 750 (m), 645 (s), 599 (s), 567 (s), 502 (s), 493 (s), 444 (s); $[Eu_2(H_2O)_6(C_5H_6O_4)(SO_4)_2]_n$ (**3**) Yield: 44%. FT-IR (ATR, ν, cm^{-1}): 3377 (m), 3233 (w), 2945 (w), 2838 (w), 2353 (w), 2306 (w), 2082 (w), 1622 (m), 1538 (s), 1442 (s), 1356(m), 1331 (w), 1264 (m), 1258 (w), 1108 (vs), 1104 (vs), 792 (m), 790 (w), 745 (w), 645 (s), 598 (vs), 503 (s), 493 (s), 474 (s); $[Gd_2(H_2O)_6(C_5H_6O_4)(SO_4)_2]_n$ (**3**) Yield: 38%. Analysis calcd for complex **3**: C, 8.06%; H, 2.44%; found: C, 8.05%; H, 2.46%. FT-IR (ATR, ν, cm^{-1}): 3377 (m), 3235 (m), 2948 (w), 2854 (w), 2353 (w), 2301 (w), 2212 (w), 2188 (w), 2082 (w), 2071 (w), 1984 (w), 1917 (w), 1623 (m), 1538 (s), 1443 (s), 1356 (m), 1332 (w), 1265 (m), 1229 (w), 1108 (vs), 1084 (vs), 964 (m), 870 (w), 792 (m), 752 (m), 646 (s), 598 (s), 493 (s).

Crystal Data Collection and Refinement. Suitable crystals of **2a** and **5** (Gd) were selected and collected on a Rigaku XtaLAB diffractometer (Mo Kα) with a HyPix 6000HE detector. The crystals were kept at 293 K for **2a** and at 298 K for **5** during data collection. Using Olex2, the structure was solved with the ShelXT structure solution program using Intrinsic Phasing and refined with the ShelXL refinement package using least-squares minimization.[55−57]

■ ASSOCIATED CONTENT

Supporting Information

The Supporting Information is available free of charge at https://pubs.acs.org/doi/10.1021/acsomega.3c08506.

Crystallographic data of **2a** (CIF)

Crystallographic data of **5** (CIF)

Selected bond distances in **2**, selected bond distances in **2a**, selected bond distances in **5**, hydrogen bond parameters for **5**; hydrogen bond parameters for **2a**; IR spectra of **1**, **2**, **2a**, **3**, **4**, and **5**, and TGA and DTA of **2** (PDF)

■ AUTHOR INFORMATION

Corresponding Authors

Saranphong Yimklan − *Department of Chemistry, Faculty of Science and Center of Excellence in Materials Science and Technology, Chiang Mai University, Chiang Mai 50200, Thailand;* orcid.org/0000-0003-4008-0845; Email: Saranphong.Yimklan@cmu.ac.th

Yothin Chimupala − *Research Laboratory of Pollution Treatment and Environmental Materials, Department of Industrial Chemistry, Faculty of Science and Center of Excellence in Materials Science and Technology, Chiang Mai University, Chiang Mai 50200, Thailand;* orcid.org/0000-0001-5634-2980; Email: Yothin.Chimupala@cmu.ac.th

Authors

Nippich Kaeosamut − *Department of Chemistry, Faculty of Science and Engineering, University of Manchester, Manchester M13 9PL, U.K.;* orcid.org/0000-0003-4574-5527

Nithiwat Sammawipawekul − *Department of Chemistry, Faculty of Science, Chiang Mai University, Chiang Mai 50200, Thailand;* orcid.org/0000-0002-5268-5086

Sutsiri Wongngam − *Department of Chemistry, Faculty of Science, Chiang Mai University, Chiang Mai 50200, Thailand*

Satienrapong Ngamsomrit − *Office of Research Administration, Chiang Mai University, Chiang Mai 50200, Thailand*

Apinpus Rujiwatra − *Department of Chemistry, Faculty of Science and Center of Excellence in Materials Science and Technology, Chiang Mai University, Chiang Mai 50200, Thailand;* orcid.org/0000-0002-2364-4592

Complete contact information is available at: https://pubs.acs.org/10.1021/acsomega.3c08506

Author Contributions

#S.Y. and N.K. contributed equally to this paper as co-first authors. S.Y. and Y.C. contributed equally to this paper as co-corresponding authors.

Notes

The authors declare no competing financial interest.

■ ACKNOWLEDGMENTS

This research was partially supported by the Faculty of Science, Chiang Mai University and the NSRF via the Program Management Unit for Human Resources and Institutional Development, Research, and Innovation [Grant number B37G660018]. The authors would like to thank W. Booncharoen and C. Phromma for their chemical and physical analysis services. S.Y. and Y.C. acknowledge the Development and Promotion of Science and Technology Talent Project (DPST) through a research fund for graduates with first placement.

■ REFERENCES

(1) Kuppler, R. J.; Timmons, D. J.; Fang, Q.-R.; Li, J.-R.; Makal, T. A.; Young, M. D.; Yuan, D.; Zhao, D.; Zhuang, W.; Zhou, H.-C. Potential Applications of Metal-Organic Frameworks. *Coord. Chem. Rev.* **2009**, *253* (23−24), 3042−3066.

(2) Bavykina, A.; Kolobov, N.; Khan, I. S.; Bau, J. A.; Ramirez, A.; Gascon, J. Metal−Organic Frameworks in Heterogeneous Catalysis: Recent Progress, New Trends, and Future Perspectives. *Chem. Rev.* **2020**, *120* (16), 8468−8535.

(3) Liu, L.; Han, Z.-B.; Wang, S.-M.; Yuan, D.-Q.; Ng, S. W. Robust Molecular Bowl-Based Metal−Organic Frameworks with Open Metal Sites: Size Modulation To Increase the Catalytic Activity. *Inorg. Chem.* **2015**, *54* (8), 3719−3721.

(4) Usman, M.; Iqbal, N.; Noor, T.; Zaman, N.; Asghar, A.; Abdelnaby, M. M.; Galadima, A.; Helal, A. Advanced Strategies in Metal-Organic Frameworks for CO_2 Capture and Separation. *Chem. Rec.* **2022**, *22*, No. e202100230.

(5) Sahoo, R.; Mondal, S.; Mukherjee, D.; Das, M. C. Metal−Organic Frameworks for CO_2 Separation from Flue and Biogas Mixtures. *Adv. Funct. Mater.* **2022**, *32* (45), 1.

(6) Thorarinsdottir, A. E.; Harris, T. D. Metal−Organic Framework Magnets. *Chem. Rev.* **2020**, *120* (16), 8716−8789.

(7) Lahcen, A. A.; Surya, S. G.; Beduk, T.; Vijjapu, M. T.; Lamaoui, A.; Durmus, C.; Timur, S.; Shekhah, O.; Mani, V.; Amine, A.; Eddaoudi, M.; Salama, K. N. Metal−Organic Frameworks Meet Molecularly Imprinted Polymers: Insights and Prospects for Sensor

Applications. *ACS Appl. Mater. Interfaces* **2022**, *14* (44), 49399−49424.
(8) Park, C.; Baek, J. W.; Shin, E.; Kim, I.-D. Two-Dimensional Electrically Conductive Metal−Organic Frameworks as Chemiresistive Sensors. *ACS Nanoscience Au* **2023**, *3* (5), 353−374.
(9) Peng, X.; Wu, X.; Zhang, M.; Yuan, H. Metal−Organic Framework Coated Devices for Gas Sensing. *ACS Sens* **2023**, *8* (7), 2471−2492.
(10) Cui, Y.; Yue, Y.; Qian, G.; Chen, B. Luminescent Functional Metal−Organic Frameworks. *Chem. Rev.* **2012**, *112* (2), 1126−1162.
(11) Zhao, Y.; Zeng, H.; Zhu, X.-W.; Lu, W.; Li, D. Metal−Organic Frameworks as Photoluminescent Biosensing Platforms: Mechanisms and Applications. *Chem. Soc. Rev.* **2021**, *50* (7), 4484−4513.
(12) Lin, R.; Liu, S.; Ye, J.; Li, X.; Zhang, J. Photoluminescent Metal−Organic Frameworks for Gas Sensing. *Adv. Sci.* **2016**, *3* (7), No. 1500434.
(13) Dong, J.; Zhao, D.; Lu, Y.; Sun, W.-Y. Photoluminescent Metal−Organic Frameworks and Their Application for Sensing Biomolecules. *J. Mater. Chem. A Mater.* **2019**, *7* (40), 22744−22767.
(14) Muecke, G. K.; Möller, P. The Not-So-Rare Earths. *Sci. Am.* **1988**, *258* (1), 72−77.
(15) Biswas, S.; Neugebauer, P. Lanthanide-Based Metal-Organic-Frameworks for Proton Conduction and Magnetic Properties. *Eur. J. Inorg. Chem.* **2021**, *2021* (45), 4610−4618.
(16) Sahoo, S.; Mondal, S.; Sarma, D. Luminescent Lanthanide Metal Organic Frameworks (LnMOFs): A Versatile Platform towards Organomolecule Sensing. *Coord. Chem. Rev.* **2022**, *470*, No. 214707.
(17) Pagis, C.; Ferbinteanu, M.; Rothenberg, G.; Tanase, S. Lanthanide-Based Metal Organic Frameworks: Synthetic Strategies and Catalytic Applications. *ACS Catal.* **2016**, *6* (9), 6063−6072.
(18) Zhang, Y.; Liu, S.; Zhao, Z.-S.; Wang, Z.; Zhang, R.; Liu, L.; Han, Z.-B. Recent Progress in Lanthanide Metal−Organic Frameworks and Their Derivatives in Catalytic Applications. *Inorg. Chem. Front* **2021**, *8* (3), 590−619.
(19) Yan, B. Luminescence Response Mode and Chemical Sensing Mechanism for Lanthanide-Functionalized Metal−Organic Framework Hybrids. *Inorg. Chem. Front* **2021**, *8* (1), 201−233.
(20) Stock, N.; Biswas, S. Synthesis of Metal-Organic Frameworks (MOFs): Routes to Various MOF Topologies, Morphologies, and Composites. *Chem. Rev.* **2012**, *112* (2), 933−969.
(21) Cook, T. R.; Zheng, Y.-R.; Stang, P. J. Metal−Organic Frameworks and Self-Assembled Supramolecular Coordination Complexes: Comparing and Contrasting the Design, Synthesis, and Functionality of Metal−Organic Materials. *Chem. Rev.* **2013**, *113* (1), 734−777.
(22) Thorarinsdottir, A. E.; Harris, T. D. Metal−Organic Framework Magnets. *Chem. Rev.* **2020**, *120* (16), 8716−8789.
(23) Zhao, Y.; Li, D. Lanthanide-Functionalized Metal−Organic Frameworks as Ratiometric Luminescent Sensors. *J. Mater. Chem. C Mater.* **2020**, *8* (37), 12739−12754.
(24) Biswas, S.; Neugebauer, P. Lanthanide-Based Metal-Organic-Frameworks for Proton Conduction and Magnetic Properties. *Eur. J. Inorg. Chem.* **2021**, *2021* (45), 4610−4618.
(25) Zhang, Y.; Liu, S.; Zhao, Z.-S.; Wang, Z.; Zhang, R.; Liu, L.; Han, Z.-B. Recent Progress in Lanthanide Metal−Organic Frameworks and Their Derivatives in Catalytic Applications. *Inorg. Chem. Front* **2021**, *8* (3), 590−619.
(26) Tan, X.-F.; Zhou, J.; Zou, H.-H.; Fu, L.; Tang, Q.; Wang, P. A Series of Lanthanide Glutarates: Lanthanide Contraction Effect on Crystal Frameworks of Lanthanide Glutarates. *RSC Adv.* **2017**, *7* (29), 17934−17940.
(27) Yang, X.; Schipper, D.; Jones, R. A.; Lytwak, L. A.; Holliday, B. J.; Huang, S. Anion-Dependent Self-Assembly of Near-Infrared Luminescent 24- and 32-Metal Cd−Ln Complexes with Drum-like Architectures. *J. Am. Chem. Soc.* **2013**, *135* (23), 8468−8471.
(28) Binnemans, K. Lanthanide-Based Luminescent Hybrid Materials. *Chem. Rev.* **2009**, *109* (9), 4283−4374.
(29) Cui, Y.; Chen, B.; Qian, G. Lanthanide Metal-Organic Frameworks for Luminescent Sensing and Light-Emitting Applications. *Coord. Chem. Rev.* **2014**, *273*−*274*, 76−86.
(30) Cui, Y.; Yue, Y.; Qian, G.; Chen, B. Luminescent Functional Metal−Organic Frameworks. *Chem. Rev.* **2012**, *112* (2), 1126−1162.
(31) Meyer, L. V.; Schönfeld, F.; Müller-Buschbaum, K. Lanthanide Based Tuning of Luminescence in MOFs and Dense Frameworks − from Mono- and Multimetal Systems to Sensors and Films. *Chem. Commun.* **2014**, *50* (60), 8093.
(32) Liu, L.; Zhang, X.-N.; Han, Z.-B.; Gao, M.-L.; Cao, X.-M.; Wang, S.-M. An In^{III} -Based Anionic Metal−Organic Framework: Sensitization of Lanthanide (III) Ions and Selective Absorption and Separation of Cationic Dyes. *J. Mater. Chem. A Mater.* **2015**, *3* (27), 14157−14164.
(33) Seoane, B.; Castellanos, S.; Dikhtiarenko, A.; Kapteijn, F.; Gascon, J. Multi-Scale Crystal Engineering of Metal Organic Frameworks. *Coord. Chem. Rev.* **2016**, *307*, 147−187.
(34) Bitzer, J.; Kleist, W. Synthetic Strategies and Structural Arrangements of Isoreticular Mixed-Component Metal−Organic Frameworks. *Chem. − .Eur. J.* **2019**, *25* (8), 1866−1882.
(35) Kaeosamut, N.; Chimupala, Y.; Yimklan, S. Anion-Controlled Synthesis of Enantiomeric Twofold Interpenetrated 3D Zinc(II) Coordination Polymer with Ligand Substitution-Induced Single-Crystal-to-Single-Crystal Transformation and Photocatalysis. *Cryst. Growth Des* **2021**, *21* (5), 2942−2953.
(36) Kim, H.-C.; Mitra, S.; Veerana, M.; Lim, J.-S.; Jeong, H.-R.; Park, G.; Huh, S.; Kim, S.-J.; Kim, Y. Cobalt(II)-Coordination Polymers Containing Glutarates and Bipyridyl Ligands and Their Antifungal Potential. *Sci. Rep.* **2019**, *9* (1), 14983.
(37) Bezuidenhout, C. X.; Smith, V. J.; Esterhuysen, C.; Barbour, L. J. Solvent- and Pressure-Induced Phase Changes in Two 3D Copper Glutarate-Based Metal−Organic Frameworks via Glutarate (+ *Gauche* ⇄ − *Gauche*) Conformational Isomerism. *J. Am. Chem. Soc.* **2017**, *139* (16), 5923−5929.
(38) Zehnder, R. A.; Jenkins, J.; Zeller, M.; Dempsey, C.; Kozimor, S. A.; Jackson, G.; Gilbert, K.; Smith, M. Conversion of Lanthanide Glutarate Chlorides with Interstitial THF into Lanthanide Glutarates with Unprecedented Topologies. *Inorg. Chim. Acta* **2018**, *471*, 502−512.
(39) Hussain, S.; Khan, I. U.; Harrison, W. T. A.; Tahir, M. N. Crystal Structures and Characterization of Two Rare-Earth-Glutarate Coordination Networks: One-Dimensional $[Nd(C_5H_6O_4)(H_2O)_4]\cdot Cl$ and Three-Dimensional $[Pr(C_5H_6O_4)(C_5H_7O_4)(H_2O)]\cdot H_2O$. *Journal of Structural Chemistry* **2015**, *56* (5), 934−941.
(40) Legendziewicz, J.; Keller, B.; Turowska-Tyrk, I.; Wojciechowski, W. Synthesis, Optical and Magnetic Properties of Homo- and Heteronuclear Systems and Glasses Containing Them. *New J. Chem.* **1999**, *23* (11), 1097−1103.
(41) Głowiak, T.; Ngoan, D.-C.; Legendziewicz, J. Structure of Diaquatriglutaratodineodymium(III) Dihydrate. *Acta Crystallogr. C* **1986**, *42* (11), 1494−1496.
(42) Stein, G.; Würzberg, E. Energy Gap Law in the Solvent Isotope Effect on Radiationless Transitions of Rare Earth Ions. *J. Chem. Phys.* **1975**, *62* (1), 208−213.
(43) Haas, Y.; Stein, G. Pathways of Radiative and Radiationless Transitions in Europium(III) Solutions. The Role of High Energy Vibrations. *J. Phys. Chem.* **1971**, *75* (24), 3677−3681.
(44) Hou, K.-L.; Bai, F.-Y.; Xing, Y.-H.; Wang, J.-L.; Shi, Z. Synthesis, Structure and Luminescence of a New Series of Rigid−Flexible Lanthanide Coordination Polymers Constructed from Benzene Sulfonic Acid and Glutaric Acid. *Inorg. Chim. Acta* **2011**, *365* (1), 269−276.
(45) Girginova, P. I.; Almeida Paz, F. A.; Soares-Santos, P. C. R.; Sá Ferreira, R. A.; Carlos, L. D.; Amaral, V. S.; Klinowski, J.; Nogueira, H. I. S.; Trindade, T. Synthesis, Characterisation and Luminescent Properties of Lanthanide-Organic Polymers with Picolinic and Glutaric Acids. *Eur. J. Inorg. Chem.* **2007**, *2007* (26), 4238−4246.
(46) Hu, D.-X.; Luo, F.; Che, Y.-X.; Zheng, J.-M. Construction of Lanthanide Metal−Organic Frameworks by Flexible Aliphatic

https://doi.org/10.1021/acsomega.3c08506
ACS Omega 2024, 9, 3988−3996

Dicarboxylate Ligands Plus a Rigid *m*-Phthalic Acid Ligand. *Cryst. Growth Des* **2007**, *7* (9), 1733−1737.
(47) Yotnoi, B.; Rujiwatra, A.; Reddy, M. L. P.; Sarma, D.; Natarajan, S. Lanthanide Sulfate Frameworks: Synthesis, Structure, and Optical Properties. *Cryst. Growth Des* **2011**, *11* (4), 1347−1356.
(48) Xu, J.; Su, W.; Hong, M. A Series of Lanthanide Secondary Building Units Based Metal−Organic Frameworks Constructed by Organic Pyridine-2,6-Dicarboxylate and Inorganic Sulfate. *Cryst. Growth Des* **2011**, *11* (1), 337−346.
(49) Yimklan, S.; Chimupala, Y.; Wongngam, S.; Kaeosamut, N. Crystal Structure of a Three-Dimensional Neodymium(III) Coordination Polymer, $[Nd_2(H_2O)_6(Glutarato)(SO_4)_2]_n$. *Acta Crystallogr. E Crystallogr. Commun.* **2022**, *78* (2), 159−163.
(50) Tan, Q.-H.; Wang, Y.-Q.; Guo, X.-Y.; Liu, H.-T.; Liu, Z.-L. A Gadolinium MOF Acting as a Multi-Responsive and Highly Selective Luminescent Sensor for Detecting *o*-, *m*-, and *p*-Nitrophenol and Fe^{3+} Ions in the Aqueous Phase. *RSC Adv.* **2016**, *6* (66), 61725−61731.
(51) Kumar, M.; Wu, L.-H.; Kariem, M.; Franconetti, A.; Sheikh, H. N.; Liu, S.-J.; Sahoo, S. C.; Frontera, A. A Series of Lanthanide-Based Metal−Organic Frameworks Derived from Furan-2,5-Dicarboxylate and Glutarate: Structure-Corroborated Density Functional Theory Study, Magnetocaloric Effect, Slow Relaxation of Magnetization, and Luminescent Properties. *Inorg. Chem.* **2019**, *58* (12), 7760−7774.
(52) Yang, H.; Xu, C.; Li, Z.; Li, M.; Liu, G. Synthesis, Characterization and Optical Properties of Three Novel Lanthanide Sulfates. *J. Solid State Chem.* **2021**, *303*, No. 122481.
(53) Strasser, A.; Vogler, A. Phosphorescence of Gadolinium(III) Chelates under Ambient Conditions. *Inorg. Chim. Acta* **2004**, *357* (8), 2345−2348.
(54) Vogler, A.; Kunkely, H. Excited State Properties of Lanthanide Complexes: Beyond Ff States. *Inorg. Chim. Acta* **2006**, *359* (12), 4130−4138.
(55) Sheldrick, G. M. *SHELXT* − Integrated Space-Group and Crystal-Structure Determination. *Acta Crystallogr. A Found Adv.* **2015**, *71* (1), 3−8.
(56) Sheldrick, G. M. Crystal Structure Refinement with *SHELXL*. *Acta Crystallogr. C Struct Chem.* **2015**, *71* (1), 3−8.
(57) Dolomanov, O. V.; Bourhis, L. J.; Gildea, R. J.; Howard, J. A. K.; Puschmann, H. *OLEX2*: A Complete Structure Solution, Refinement and Analysis Program. *J. Appl. Crystallogr.* **2009**, *42* (2), 339−341.

https://doi.org/10.1021/acsomega.3c08506
ACS Omega 2024, 9, 3988−3996